

Article

Fabrication of ZnWO₄-SnO₂ Core–Shell Nanorods for Enhanced Solar Light-Driven Photoelectrochemical Performance

Bathula Babu ¹, Shaik Gouse Peera ^{2,*} and Kisoo Yoo ^{1,*}

¹ School of Mechanical Engineering, Yeungnam University, Gyeongsan 38541, Republic of Korea; babu.physicist@gmail.com

² Department of Environmental Science, Keimyung University, Daegu 42601, Republic of Korea

* Correspondence: gouse@kmu.ac.kr (S.G.P.); kisooyoo@yu.ac.kr (K.Y.)

Abstract: This article describes the effective synthesis of colloidal SnO₂ quantum dots and ZnWO₄ nanorods using wet chemical synthesis and hydrothermal synthesis, respectively. The resulting ZnWO₄-SnO₂ core–shell nanorod heterostructure is then made, and its structural, optical, and morphological properties are assessed using XRD, SEM, TEM, and DRS. The heterojunction's structural confinement increases the exposure of its reactive sites, and its electronic confinement promotes its redox activity. The heterostructure subsequently exhibits a smaller bandgap and better light-harvesting capabilities, resulting in increased photoelectrochemical performance. The heterostructure of core–shell nanorods shows promise for usage in a range of optoelectronic devices and effective solar energy conversion.

Keywords: ZnWO₄; nanorods; SnO₂; quantum dots; core–shell; photoelectrochemical

1. Introduction

Photoelectrochemical water splitting has received a lot of attention as a potential source of clean and sustainable energy. This process splits water into hydrogen and oxygen using a photoelectrochemical (PEC) cell, transforming solar energy into chemical energy [1]. Photoelectrochemical splitting has the potential for higher efficiency, scalability, and energy storage than other renewable energy sources such as the wind and the sun. Although TiO₂ has been investigated a great deal because of its remarkable qualities, including its high electron mobility, stability, and availability, its wide bandgap limits its capacity to absorb light and operate photoelectrochemically [2,3]. To overcome this limitation, other metal oxide semiconductors have been investigated, including ZnO, Fe₂O₃, WO₃, and SnO₂. Some of these materials offer narrower bandgaps, better light harvesting properties, and potential for bandgap engineering. Because of their small bandgaps, great stability, and comparatively low toxicity, Fe₂O₃ and WO₃ in particular appear attractive [4]. Due to its high electron mobility, stability, and abundance, SnO₂, while being a wide bandgap semiconductor, has demonstrated considerable potential for effective photoelectrochemical water splitting [5,6]. These materials offer the advantage of being earth-abundant, non-toxic, and chemically stable, making them attractive for large-scale applications. As a result, researching metal oxide semiconductors for photoelectrochemical water splitting offers a possible route for the creation of clean and sustainable energy [7].

Efficient and stable photoelectrochemical devices remain a significant challenge, driving ongoing research to identify new materials with enhanced photoelectrochemical performance. ZnWO₄ nanorods and SnO₂ quantum dots are emerging as promising materials for efficient photoelectrochemical water splitting due to their unique properties. ZnWO₄ has a wide bandgap, making it suitable for absorbing UV light and generating high photocurrents, while its high surface area and aspect ratio in the form of nanorods facilitate efficient charge separation and transfer [8]. Additionally, ZnWO₄ is a chemically stable and



Citation: Babu, B.; Peera, S.G.; Yoo, K. Fabrication of ZnWO₄-SnO₂ Core–Shell Nanorods for Enhanced Solar Light-Driven Photoelectrochemical Performance. *Inorganics* **2023**, *11*, 213. <https://doi.org/10.3390/inorganics11050213>

Academic Editor: Zemin Zhang

Received: 6 April 2023

Revised: 11 May 2023

Accepted: 12 May 2023

Published: 15 May 2023



Copyright: © 2023 by the authors. Licensee MDPI, Basel, Switzerland. This article is an open access article distributed under the terms and conditions of the Creative Commons Attribution (CC BY) license (<https://creativecommons.org/licenses/by/4.0/>).

earth-abundant material, making it an attractive option for large-scale production. In contrast, SnO₂ quantum dots possess a small size and high surface area, facilitating improved charge transfer and efficient light absorption. In addition to having a broad bandgap, SnO₂ may be tuned, which enables it to effectively absorb visible light and provide high photocurrent densities [9]. SnO₂ is a plentiful, non-toxic, and chemically stable substance that is also safe and sustainable for use in large-scale applications. Due to their unique characteristics, ZnWO₄ nanorods and SnO₂ quantum dots are attractive candidates for the development of efficient photoelectrochemical water-splitting systems. The use of these materials can increase photocurrent densities, improve charge separation, and facilitate the efficient absorption of light. As a result, a lot of hydrogen fuel and oxygen may be produced, which can be used as a clean, sustainable source of energy. For the development of efficient and economical photoelectrochemical water-splitting systems that can help to meet the expanding global need for clean and renewable energy, ZnWO₄ nanorods and SnO₂ quantum dots offer a possible path forward. These materials are abundant, stable, and sustainable.

In a series of studies, various novel photoanode materials and heterostructures were synthesized and characterized for ZnWO₄-based photoelectrochemical water-splitting performance. Because of its significant visible light absorption, a composite of one-dimensional ZnWO₄ nanorods and WO₃ nanoplates heterojunction was reported by Mohan Kumar et al. to exhibit outstanding PEC activity when compared to pure ZnWO₄ and WO₃ [10]. Cui et al. looked into WO₃ nanorod arrays with defective ZnWO₄ decorations for effective PEC water splitting. As a comparison to pure WO₃ nanorod arrays, type-II heterojunction nanorod arrays displayed significantly better PEC activity, with the ideal ZnWO₄ decoration and surface defects exhibiting high incident photon-to-current efficiency and relatively high photostability [11]. A unique NiFe₂O₄-ZnWO₄ nanocomposite was reported by Koutavarapu et al. to have been made using a straightforward hydrothermal method. It demonstrated strong photocurrents and charge-transfer resistance, making it a potential material for water splitting [12]. Babu et al. studied the PEC performance of a hydrothermally prepared Bi₂WO₆ nanocomposite anchored with ZnWO₄ nanorods, which exhibited low charge-transfer resistance and strong interfaces, improving its PEC performance under solar irradiation [13]. A one-dimensional ZnWO₄@SnWO₄ core-shell heterostructure was created by Zhuang et al. with improved PEC performance when exposed to visible light, which was attributed to the effective separation and transfer of photo-generated charge carriers [14]. ZnWO₄ boosted the performance of ZnO NRs-based PEC water-splitting cells by enhancing charge transfer between the photoanode and electrolyte, leading to improved PEC activity compared to the pure ZnO nanorods, according to research by Wannapop et al. [15]. Overall, these studies highlight the potential of novel photoanode materials and heterostructures for efficient PEC water splitting.

Several studies have focused on developing efficient photoelectrochemical water-splitting systems. A three-dimensional macroporous BiVO₄/SnO₂ inverse opal heterostructure with Au nanoparticles was used by Zhou et al. to build a very effective system that demonstrated a notable improvement in photoelectrochemical water-splitting performance [16]. Similarly, Bai et al. developed a ternary photoanode of SnO₂/BiVO₄/rGO, which exhibited remarkably higher photocurrent density than BiVO₄ photoanodes [17]. Three-dimensional nanoporous SnO₂/CdS heterojunction was used by Hu et al. to create a high-performance system that displayed a photocurrent density that was 9.7 times more than that of planar SnO₂/CdS films [18]. Lei et al. developed a SnO₂-TiO₂ bilayer composite film that exhibited enhanced photoelectrochemical performances by co-doping with nitrogen and fluorine [19]. Kahng et al. developed a SnO₂/Mo:BiVO₄ photoanode that exhibited outstanding photoelectrochemical performance and can be used to degrade tetracycline hydrochloride [20]. Koutavarapu et al. studied improving photoelectrochemical water oxidation by utilizing a novel nanocomposite of nickel ferrite and tin oxide quantum dots (NF-SQD) and found that it exhibited better improvement in photoelectrochemical water oxidation compared to other prepared samples [21]. For photoelectrochemical wa-

ter splitting, Babu et al. created a ternary nanocomposite named g-CN/Au-SQD that displayed a significant photocurrent and reduced charge-transfer resistance more than other generated samples [22]. They also discussed how cadmium sulfide–tin oxide quantum dots core–shell nanorods outperformed virgin cadmium sulfide nanorods in terms of photoelectrochemical performance, producing larger photocurrents and lower charge transfer resistance [23]. These findings emphasize the significance of creating effective photoelectrochemical systems for water splitting and the possibility of nanocomposites to enhance their functionality.

The present study investigates ZnWO₄-SnO₂ core–shell nanorods, which combine the properties of both materials to offer even greater photoelectrochemical performance. By utilizing both materials in the core–shell nanorod structure, the present study seeks to enhance photoelectrochemical performance even further. Overall, the development of effective and long-lasting photoelectrochemical water-splitting technology has important ramifications for the production of clean and renewable energy, and continuous research in this field offers great promise for the future.

2. Results and Discussion

2.1. Structural Analysis

The present study investigated the crystal phase of ZNR and ZW-CS nanorods using the XRD technique. The purpose of this analysis was to understand their respective properties. The XRD patterns obtained from both samples were analyzed, and the results were presented in Figure 1.

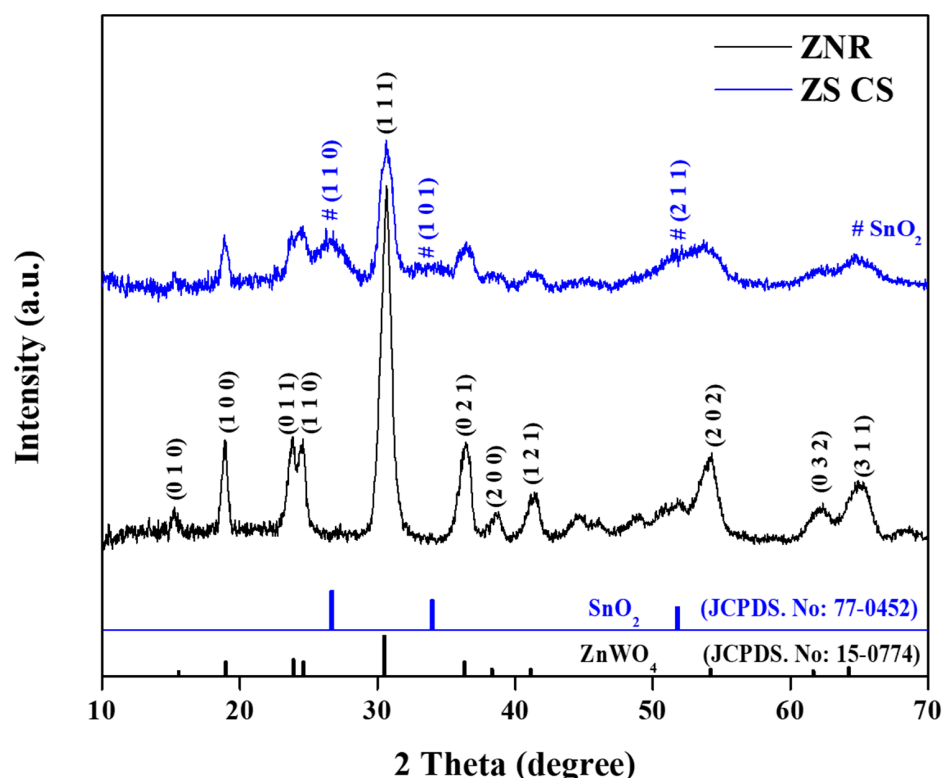


Figure 1. XRD pattern of ZNR and ZS CS nanorods.

The monoclinic zinc tungsten oxide structure was found to be present in the ZNR, and the diffraction peaks were identified as belonging to different planes (0 1 0), (1 0 0), (0 1 1), (1 1 0), (1 1 1), (0 2 1), (2 0 0), (1 2 1), (2 0 2), (0 3 2) and (3 1 1). These peaks were in good agreement with the monoclinic zinc tungsten oxide (JCPDS. No: 15-0774). The ZNR's XRD pattern revealed no impurity peaks, proving its purity. The development of a SnO₂ QD's shell around the ZnWO₄ core, however, was indicated by the XRD pattern of the ZS CS,

which displayed lower diffraction peak intensities of the ZNR [24,25]. Furthermore, the core–shell nanorod pattern and the SnO₂ QD XRD peaks both supported the development of the shell in the ZS CS sample. The (1 1 0), (1 0 1), and (2 1 1) planes of tetragonal SnO₂ were identified as the locations of the observed XRD peaks (JCPDS. No: 77-0452). The XRD peaks of the SnO₂ QD were, however, weaker than those of the ZnWO₄ nanorods. This was the case because the peak intensities of the ZNR nanorods were significantly higher than those of the SnO₂ QD. Moreover, compared to ZNR, the XRD peaks of SnO₂ QDs are often broader and less intense. It was claimed that the little quantity of colloidal SnO₂ QDs employed in the production of ZW CS nanorods would be to blame for the reduced prominence of SnO₂ QD's XRD peaks [26].

2.2. Morphological Study

The purpose of this study was to characterize the morphology of ZNR and their core–shell equivalents using TEM and SEM methods (ZS CS). The results of XRD analysis showed that the ZNR exhibited a pure monoclinic zinc tungsten oxide structure, while the ZS CS sample had a SnO₂ QD's shell on the ZnWO₄ core. SEM imaging of the as-prepared ZNR showed a smooth surface, while the surface of the ZS CS nanorods appeared to be rough due to the adsorption of SnO₂ QD's after the synthesis of the core–shell structure (Figure 2a,b). The production of ZS CS nanorods was greatly aided by the high temperature and pressure produced by the sonochemical process, which strengthened the bond between the surface of the NR and QDs. The production of the core–shell nanorods was verified by TEM and SEM pictures, which showed that the SnO₂ QDs were embellished on the ZNR core surface in the ZS CS nanorods (Figure 2c,d). The intimate interfacial contact between the ZnWO₄ and SnO₂ quantum dots, as well as the rational core–shell structure of the ZS CS nanorods, lead to improved PEC performance, which is essential for their potential application in water splitting. Nevertheless, the small islands of SnO₂ QDs in the ZS CS film may provide additional surface area and connectivity for the nanorods, which could contribute to the improved electrochemical activity to some extent.

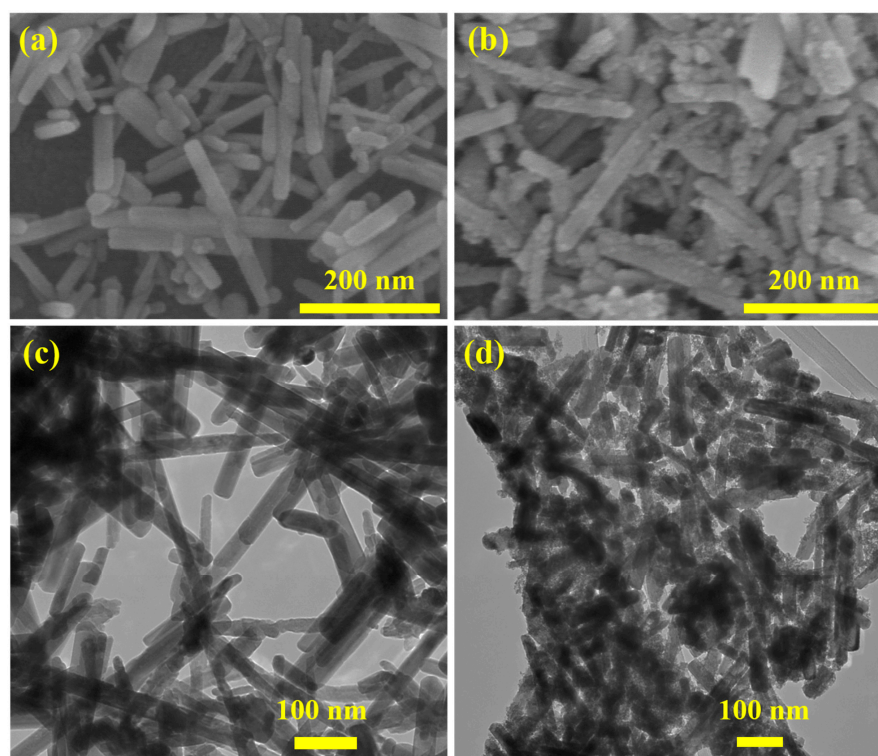


Figure 2. SEM (a) and TEM (c) images of ZNR. SEM (b) and TEM (d) images of ZS CS nanorods.

The results suggested that the surface of the ZNR was fully covered with SnO₂ QDs in the case of ZS CS nanorods. HR-TEM images and fringe patterns in Figure 3a–d depict the formation of ZS CS nanorods. Additionally, lattice fringes of ZnWO₄ and SnO₂ quantum dots on (1 1 1) and (1 1 0) planes, respectively, shown in Figure 3d, confirm the core–shell structure, with lattice fringe line distances of approximately 0.29 nm and 0.33 nm for ZnWO₄ and SnO₂, respectively. The SEM, TEM, and HR-TEM analyses all consistently support the morphology of the ZS CS nanorods. Overall, these findings provide comprehensive evidence for the formation of core–shell nanorods of ZnWO₄ and SnO₂.

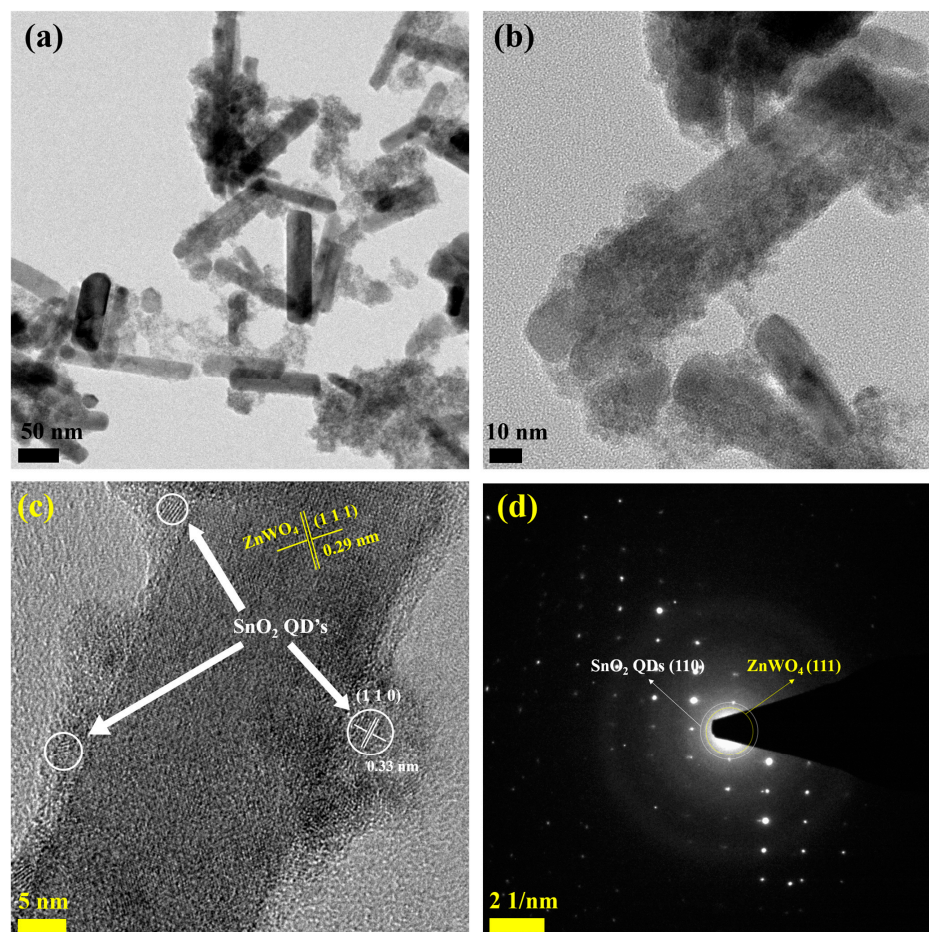


Figure 3. (a,b) HRTEM, (c) lattice fringe, and (d) SAED pattern of ZS CS nanorods.

2.3. Absorption Study

The absorption spectra presented in Figure 4 provide insights into the optical properties of ZNR and ZS CS nanorods. Whereas ZS CS nanorods displayed a wide absorption range in the UV–Visible range, ZNR’s absorption range was only seen in the UV light range. The band transition from the filled O 2p orbital to the vacant W 5d orbital is responsible for ZNR’s absorption. Yet, the development of a shell surrounding the core nanorods of ZS CS nanorods may be the cause of their high absorption, increasing their capacity for light harvesting by reducing their bandgap [24]. The bandgap value of ZNR was found to be 3.54 eV, while that of the as-synthesized colloidal SnO₂ QDs was determined to be 2.8 eV. In contrast, the bandgap of ZS CS nanorods was calculated to be 3.26 eV, indicating a decrease in bandgap compared to ZNR, which can be attributed to the formation of a shell. The formation of a shell around a core can lead to quantum confinement effects, which can result in a decrease in the bandgap [27]. The change in absorbance indicates the successful formation of ZS CS nanorods [28]. When ZnWO₄ nanorods were combined with SnO₂ QDs, the absorption peak of the ZS CS nanorods was red-shifted, indicating close

contact between the two semiconductors with appropriately matched band edges. This red-shifted absorption peak and the slight shift in absorption edge indicate the formation of a heterojunction that can improve photoelectrochemical performance [29].

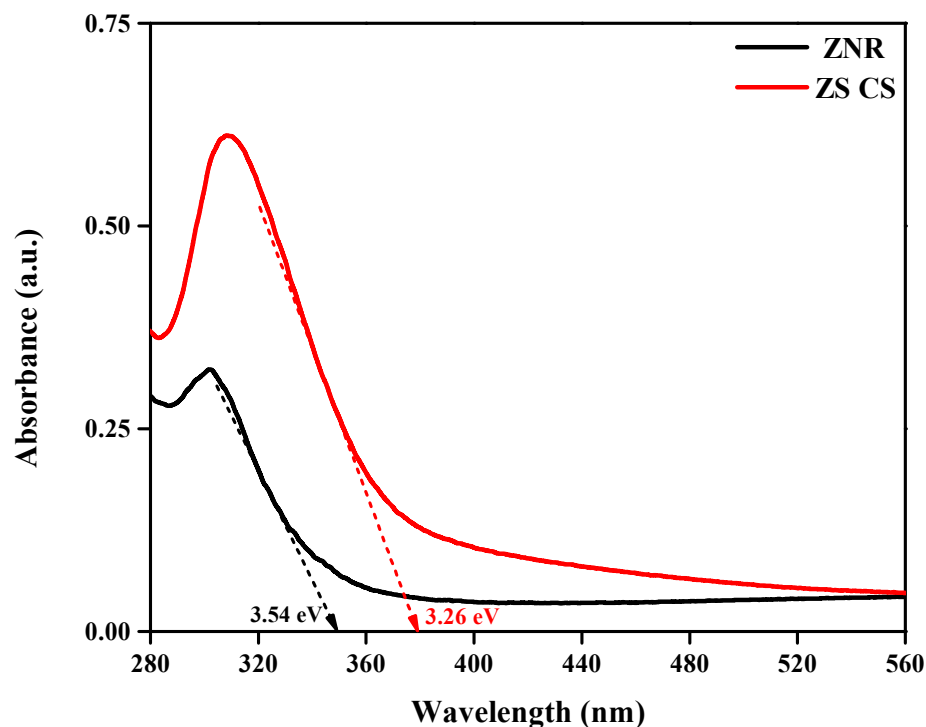


Figure 4. UV-Vis DRS spectra of ZNR and ZS CS nanorods.

In summary, the optical absorption spectra show that ZS CS nanorods were successfully formed, and the reduced bandgap has increased the ability to collect light [30]. The redshifted absorption peak and the slight shift in absorption edge indicate a tight contact between the two semiconductors and the formation of a heterojunction, respectively, which can improve the photoelectrochemical performance. These findings provide valuable insights into the optical properties of ZNR and ZS CS nanorods, which could have potential applications in photocatalytic and photovoltaic devices.

2.4. Photoelectrochemical Study

Using a three-electrode system, the PEC characteristics of photoanodes made using as-synthesized ZNR and ZS CS nanorods were examined. The results are shown in LSV in Figure 5a. Under dark, the current density seen for both ZNR and ZS CS nanorods was insignificant [31]. However, the current density of ZS CS nanorods was found to be higher than that of ZNR under light conditions, with a difference of 0.57 mA/cm^2 , i.e., 0.73 and 0.16 mA/cm^2 , respectively. The onset potential was significantly lower for ZS CS nanorods than for pristine ZNRs, as revealed by LSV. The excellent crystallinity of ZNR using a hydrothermal method and their unchanged crystallinity even after the formation of core-shell nanorods structure, the close interfacial contact between ZnWO_4 nanorods and SnO_2 QDs, which is favorable for the transfer of photogenerated electrons, and core-shell structure are the factors that contribute to the improved PEC performance [28]. The higher current density in the presence of light shows that the photoanodes can effectively split water using solar energy. The low onset potential and high photocurrent density of ZS CS nanorods confirm the effectiveness of the heterojunction formed between ZnWO_4 nanorods and SnO_2 QDs [27]. This close interfacial contact between the two semiconductors improves charge separation and prevents photo-induced charge carriers from recombining.

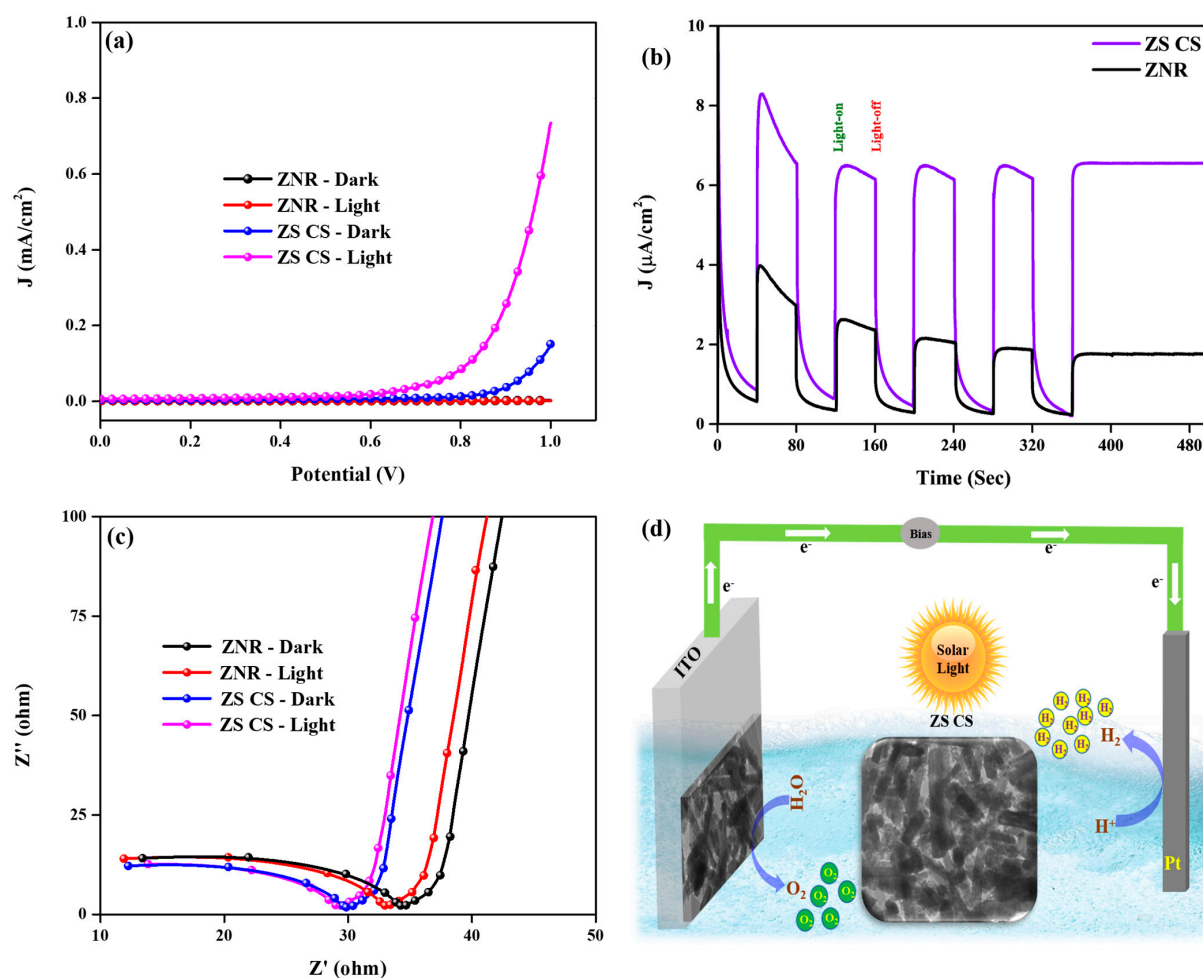


Figure 5. (a) LSV, (b) $I-t$, (c) EIS spectra of ZNR and ZS CS nanorods, and (d) PEC water-splitting mechanism of ZS CS nanorods.

Chronoamperometric $I-t$ plots were used to assess the stability of the as-synthesized ZNR and ZS CS nanorods in both light and darkness. The results are shown in Figure 5b, where it is clear that under light, ZS CS had a larger current density than virgin ZNR, indicating a quicker separation of photogenerated charge carriers. Moreover, clean ZNR and ZS CS both retained their stability for additional repeated cycles. Up to 500 s of light on and light off testing were used to evaluate the photoresponse and stability of the photoanode. The researchers used the electrochemical impedance spectroscopy (EIS) method to measure the charge transfer resistance at the electrode–electrolyte interface. Figure 5c analyzes and displays the Nyquist impedance plots of the ZNR and ZS CS photoanodes, which feature a semicircle in the high-frequency zone and a line in the low-frequency region. The smaller radius of the semicircle implies low charge transfer resistance and good electrical conductivity at the electrode–electrolyte contact, whereas the greater radius implies the opposite. The core–shell structure of ZS greatly lowered the charge transfer resistance, resulting in superior PEC performance, as evidenced by the fact that the semicircle radius of ZS CS was lower than that of pristine ZNR [32]. Additionally, the drop in the semicircle radius when the light was on demonstrated that the electrical conductivity at the contact was better in the presence of light than in the absence of light. These findings imply that over ZS CS nanorods, photogenerated carriers and photoinduced charge transfer were separated more efficiently, improving PEC performance. The observed photoelectrochemical water oxidation mechanism is shown in Figure 5d. The production of a heterostructure as a result of the photoanode being exposed to solar light caused the creation and separation of electron–hole pairs, which then took part in redox processes [27].

An oxidation process took place at the counter electrode, while a reduction reaction took place at the working electrode created by the ZS CS nanorods. It was made possible for photogenerated electrons and holes to move from the CB of ZnWO_4 to the CB of SnO_2 and from the VB of SnO_2 to the VB of ZnWO_4 , respectively, thanks to the type-II heterojunction that was created between these materials.

This transfer was caused by the two materials' inherent potential differences (Figure 6). In particular, when the photoanode is illuminated, the photogenerated electron and holes are generated in the ZS CS nanorods and ZNRs. Due to the intimate contact between ZnWO_4 and SnO_2 quantum dots and the rational core-shell structure of ZS CS nanorods, the electrons can efficiently transfer from the ZnWO_4 to SnO_2 , leading to the effective separation of electron-hole pairs. The photogenerated holes at the ZS CS nanorod surface can directly participate in the water oxidation reaction, resulting in the formation of O_2 gas. At the Pt counter electrode, where they took part in the reduction of water, they continued their journey through a wire and produces H_2 gas [10,11]. Because of the effective charge separation and transfer produced by this mechanism, the ZS CS nanorods used in the study displayed improved photoelectrochemical performance.

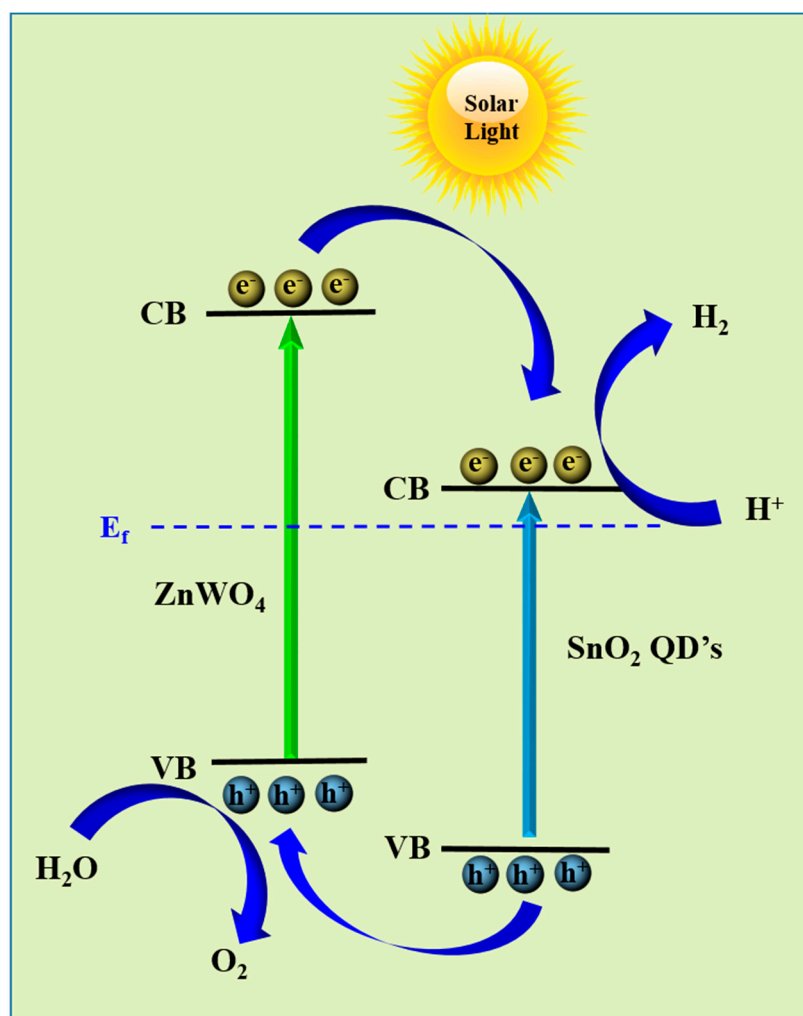


Figure 6. Charge transfer mechanism of ZS CS nanorods.

3. Experimental Section

The Supplementary Information contains details of the synthesis process for both ZnWO_4 nanorods (ZNR) and colloidal SnO_2 quantum dots (QDs). The ZnWO_4 - SnO_2 core-shell (ZS CS) nanorods were prepared by first dispersing 100 mg of ZnWO_4 nanorods

in 50 mL of ethanol and stirring for 30 min. Subsequently, the ZnWO₄ nanorods were gradually mixed with 1 mL of colloidal SnO₂ QDs and exposed to ultrasonic waves for 2 h. The final product was purified through a washing and centrifugation process and dried at a temperature of 80 °C for 12 h. The additional information related to characterizations and PEC experimental procedure is provided in the Supporting Information.

4. Conclusions

For the purpose of photoelectrochemical water splitting, our work investigated the potential of ZnWO₄-SnO₂ core-shell (ZS CS) nanorods as a photoanode material. Through XRD analysis, we confirmed the formation of the ZS CS nanorods with a crystalline structure. The ZS CS nanorods' improved light harvesting capacity is owing to their core-shell structure, which is demonstrated by the UV-Vis absorption analysis to have significantly increased the absorption of visible light. SEM and TEM morphology examinations shed light on the size and shape of the nanorods. EIS analysis revealed that the ZS CS nanorods had decreased charge-transfer resistance and increased electrical conductivity at the electrode-electrolyte interface, all of which are necessary for improved photoelectrochemical performance. The produced ZS CS nanorods performed predictably and at a high rate of separation of photogenerated charge carriers, with a larger current density seen in the presence of light, according to chronoamperometric *I-t* plots. The observed photoelectrochemical water oxidation mechanism revealed the formation and separation of electron-hole pairs, their involvement in redox reactions, and the contribution of ultrasonic energy to the formation of a core-shell structure. Overall, our results indicate that the ZS CS nanorods, because of their improved light collecting ability, effective charge separation and transfer, and stable performance under light, have tremendous potential as a photoanode material for photoelectrochemical water splitting.

Supplementary Materials: The following supporting information can be downloaded at: <https://www.mdpi.com/article/10.3390/inorganics11050213/s1>.

Author Contributions: Conceptualization, methodology, validation, writing—original draft preparation: B.B.; formal analysis, resources, data curation, and writing—original draft preparation: S.G.P.; supervision, project administration, and funding acquisition: K.Y. All authors have read and agreed to the published version of the manuscript.

Funding: This work was supported by the National Research Foundation of Korea (NRF) grant funded by the Korean Government (MSIT) (No. 2021R1C1C1011089).

Institutional Review Board Statement: Not applicable.

Informed Consent Statement: Not applicable.

Data Availability Statement: The data that support the findings of this study are available from the corresponding author, upon reasonable request.

Conflicts of Interest: The authors declare that they have no conflict of interest regarding the publication of this article, financial and/or otherwise.

References

1. Kumar, M.; Meena, B.; Subramanyam, P.; Suryakala, D.; Subrahmanyam, C. Recent trends in photoelectrochemical water splitting: The role of cocatalysts. *NPG Asia Mater.* **2022**, *14*, 88. [CrossRef]
2. Ghayeb, Y.; Momeni, M.M.; Shafiei, M. WO₃-TiO₂ nanotubes modified with tin oxide as efficient and stable photocatalysts for photoelectrochemical water splitting. *J. Iran Chem. Soc.* **2020**, *17*, 1131–1140. [CrossRef]
3. Li, P.; Liu, M.; Li, J.; Guo, J.; Zhou, Q.; Zhao, X.; Wang, S.; Wang, L.; Wang, J.; Chen, Y.; et al. Atomic heterojunction-induced accelerated charge transfer for boosted photocatalytic hydrogen evolution over 1D CdS nanorod/2D ZnIn₂S₄ nanosheet composites. *J. Colloid Interface Sci.* **2021**, *604*, 500–507. [CrossRef] [PubMed]
4. Huang, Y.-C.; Li, Y.; Arul, K.T.; Ohigashi, T.; Nga, T.T.T.; Lu, Y.-R.; Chen, C.-L.; Chen, J.-L.; Shen, S.; Pong, W.-F.; et al. Atomic Nickel on Graphitic Carbon Nitride as a Visible Light-Driven Hydrogen Production Photocatalyst Studied by X-ray Spectromicroscopy. *ACS Sustain. Chem. Eng.* **2023**, *11*, 5390–5399. [CrossRef]

5. Babu, B.; Talluri, B.; Gurugubelli, T.R.; Kim, J.; Yoo, K. Effect of annealing environment on the photoelectrochemical water oxidation and electrochemical supercapacitor performance of SnO₂ quantum dots. *Chemosphere* **2022**, *286*, 131577. [[CrossRef](#)]
6. Huang, Y.-C.; Chen, J.; Lu, Y.-R.; Arul, K.T.; Ohigashi, T.; Chen, J.-L.; Chen, C.-L.; Shen, S.; Chou, W.-C.; Pong, W.-F.; et al. Single-atom cobalt-incorporating carbon nitride for photocatalytic solar hydrogen conversion: An X-ray spectromicroscopy study. *J. Electron Spectrosc. Relat. Phenom.* **2023**, *264*, 147319. [[CrossRef](#)]
7. Nga, T.T.T.; Huang, Y.-C.; Chen, J.-L.; Chen, C.-L.; Lin, B.-H.; Yeh, P.-H.; Du, C.-H.; Chiou, J.-W.; Pong, W.-F.; Arul, K.T.; et al. Effect of Ag-Decorated BiVO₄ on Photoelectrochemical Water Splitting: An X-ray Absorption Spectroscopic Investigation. *Nanomaterials* **2022**, *12*, 3659. [[CrossRef](#)]
8. Abubakar, H.L.; Tijani, J.O.; Abdulkareem, S.A.; Mann, A.; Mustapha, S. A review on the applications of zinc tungstate (ZnWO₄) photocatalyst for wastewater treatment. *Heliyon* **2022**, *8*, e09964. [[CrossRef](#)]
9. Sun, M.; Gong, Z.; Zhang, Z.; Li, Y.; Xie, D.; Wu, F.; Li, R. Dependence of photoelectrochemical water splitting for oriented-SnO₂ on Carrier behaviors: Concentration, depletion and transportation. *Thin Solid Films* **2021**, *732*, 138794. [[CrossRef](#)]
10. Kumar, G.M.; Lee, D.J.; Jeon, H.C.; Ilanchezhian, P.; Young, K.D.; Won, K.T. One dimensional ZnWO₄ nanorods coupled with WO₃ nanoplates heterojunction composite for efficient photocatalytic and photoelectrochemical activity. *Ceram. Int.* **2022**, *48*, 4332–4340. [[CrossRef](#)]
11. Cui, Y.; Pan, L.; Chen, Y.; Afzal, N.; Ullah, S.; Liu, D.; Wang, L.; Zhang, X.; Zou, J.-J. Defected ZnWO₄-decorated WO₃ nanorod arrays for efficient photoelectrochemical water splitting. *RSC Adv.* **2019**, *9*, 5492–5500. [[CrossRef](#)]
12. Reddy, C.V.; Koutavarapu, R.; Reddy, K.R.; Shetti, N.P.; Aminabhavi, T.M.; Shim, J. Z-scheme binary 1D ZnWO₄ nanorods decorated 2D NiFe₂O₄ nanoplates as photocatalysts for high efficiency photocatalytic degradation of toxic organic pollutants from wastewater. *J. Environ. Manag.* **2020**, *268*, 110677. [[CrossRef](#)]
13. Babu, B.; Koutavarapu, R.; Shim, J.; Kim, J.; Yoo, K. Enhanced solar-light-driven photocatalytic and photoelectrochemical properties of zinc tungsten oxide nanorods anchored on bismuth tungsten oxide nanoflakes. *Chemosphere* **2021**, *268*, 129346. [[CrossRef](#)]
14. Zhuang, H.; Xu, W.; Lin, L.; Huang, M.; Xu, M.; Chen, S.; Cai, Z. Construction of one dimensional ZnWO₄@SnWO₄ core-shell heterostructure for boosted photocatalytic performance. *J. Mater. Sci. Technol.* **2019**, *35*, 2312–2318. [[CrossRef](#)]
15. Wannapop, S.; Somdee, A. Effect of citric acid on the synthesis of ZnWO₄/ZnO nanorods for photoelectrochemical water splitting. *Inorg. Chem. Commun.* **2020**, *115*, 107857. [[CrossRef](#)]
16. Zhou, S.J.; Tang, R.; Zhang, L.Y.; Yin, L.W. Au Nanoparticles coupled Three-dimensional Macroporous BiVO₄/SnO₂ Inverse Opal Heterostructure For Efficient Photoelectrochemical Water Splitting. *Electrochim. Acta* **2017**, *248*, 593–602. [[CrossRef](#)]
17. Bai, S.L.; Tian, K.; Meng, J.C.; Zhao, Y.Y.; Sun, J.H.; Zhang, K.W.; Feng, Y.J.; Luo, R.X.; Li, D.Q.; Chen, A.F. Reduced graphene oxide decorated SnO₂/BiVO₄ photoanode for photoelectrochemical water splitting. *J. Alloys Compd.* **2021**, *855*, 10. [[CrossRef](#)]
18. Hu, W.G.; Quang, N.D.; Majumder, S.; Jeong, M.J.; Park, J.H.; Cho, Y.J.; Kim, S.B.; Lee, K.; Kim, D.; Chang, H.S. Three-dimensional nanoporous SnO₂/CdS heterojunction for high-performance photoelectrochemical water splitting. *Appl. Surf. Sci.* **2021**, *560*, 10. [[CrossRef](#)]
19. Lei, C.X.; Huang, X.; Liu, X.; Wang, L.S.; Zhang, G.S.; Peng, D.L. Photoelectrochemical performances of the SnO₂-TiO₂ bilayer composite films prepared by a facile liquid phase deposition method. *J. Alloys Compd.* **2017**, *692*, 227–235. [[CrossRef](#)]
20. Kahng, S.; Kim, J.H. Heterojunction photoanode of SnO₂ and Mo-doped BiVO₄ for boosting photoelectrochemical performance and tetracycline hydrochloride degradation. *Chemosphere* **2022**, *291*, 10. [[CrossRef](#)]
21. Babu, B.; Koutavarapu, R.; Shim, J.; Kim, J.; Yoo, K. Improved sunlight-driven photocatalytic abatement of tetracycline and photoelectrocatalytic water oxidation by tin oxide quantum dots anchored on nickel ferrite nanoplates. *J. Electroanal. Chem.* **2021**, *900*, 115699. [[CrossRef](#)]
22. Babu, B.; Koutavarapu, R.; Shim, J.; Yoo, K. Enhanced visible-light-driven photoelectrochemical and photocatalytic performance of Au-SnO₂ quantum dot-anchored g-C₃N₄ nanosheets. *Sep. Purif. Technol.* **2020**, *240*, 15. [[CrossRef](#)]
23. Babu, B.; Kim, J.; Yoo, K. Improved solar light-driven photoelectrochemical performance of cadmium sulfide-tin oxide quantum dots core-shell nanorods. *Mater. Lett.* **2020**, *274*, 4. [[CrossRef](#)]
24. Ranjith, K.S.; Castillo, R.B.; Sillanpaa, M.; Rajendra Kumar, R.T. Effective shell wall thickness of vertically aligned ZnO-ZnS core-shell nanorod arrays on visible photocatalytic and photo sensing properties. *Appl. Catal. B Environ.* **2018**, *237*, 128–139. [[CrossRef](#)]
25. Guo, X.; Li, M.; Liu, Y.; Huang, Y.; Geng, S.; Yang, W.; Yu, Y. Hierarchical core-shell electrode with NiWO₄ nanoparticles wrapped MnCo₂O₄ nanowire arrays on Ni foam for high-performance asymmetric supercapacitors. *J. Colloid Interface Sci.* **2020**, *563*, 405–413. [[CrossRef](#)]
26. Ravi, P.; Navakoteswara Rao, V.; Shankar, M.V.; Sathish, M. CuO@NiO core-shell nanoparticles decorated anatase TiO₂ nanospheres for enhanced photocatalytic hydrogen production. *Int. J. Hydrogen Energy* **2020**, *45*, 7517–7529. [[CrossRef](#)]
27. Kumar, S.; Ganguli, A.K. Enhanced photoelectrochemical water splitting and mitigation of organic pollutants under visible light with NaNbO₃@CuS Core-Shell heterostructures. *Appl. Surf. Sci. Adv.* **2022**, *9*, 10. [[CrossRef](#)]
28. Kumar, S.; Malik, T.; Sharma, D.; Ganguli, A.K. NaNbO₃/MoS₂ and NaNbO₃/BiVO₄ Core-Shell Nanostructures for Photoelectrochemical Hydrogen Generation. *ACS Appl. Nano Mater.* **2019**, *2*, 2651–2662. [[CrossRef](#)]
29. Mendhe, A.C.; Majumder, S.; Nair, N.; Sankapal, B.R. Core-shell cadmium sulphide @ silver sulphide nanowires surface architecture: Design towards photoelectrochemical solar cells. *J. Colloid Interface Sci.* **2021**, *587*, 715–726. [[CrossRef](#)]

30. Mahajan, P.; Singh, A.; Arya, S. Improved performance of solution processed organic solar cells with an additive layer of sol-gel synthesized ZnO/CuO core/shell nanoparticles. *J. Alloys Compd.* **2020**, *814*, 152292. [[CrossRef](#)]
31. Park, J.; Deshmukh, P.R.; Sohn, Y.; Shin, W.G. ZnO-TiO₂ core-shell nanowires decorated with Au nanoparticles for plasmon-enhanced photoelectrochemical water splitting. *J. Alloys Compd.* **2019**, *787*, 1310–1319. [[CrossRef](#)]
32. Koutavarapu, R.; Reddy, C.V.; Syed, K.; Reddy, K.R.; Saleh, T.A.; Lee, D.-Y.; Shim, J.; Aminabhavi, T.M. Novel Z-scheme binary zinc tungsten oxide/nickel ferrite nanohybrids for photocatalytic reduction of chromium (Cr (VI)), photoelectrochemical water splitting and degradation of toxic organic pollutants. *J. Hazard. Mater.* **2022**, *423*, 127044. [[CrossRef](#)] [[PubMed](#)]

Disclaimer/Publisher's Note: The statements, opinions and data contained in all publications are solely those of the individual author(s) and contributor(s) and not of MDPI and/or the editor(s). MDPI and/or the editor(s) disclaim responsibility for any injury to people or property resulting from any ideas, methods, instructions or products referred to in the content.